Black-hole production from ultrarelativistic collisions

FAST TRACK COMMUNICATION

Black-hole production from ultrarelativistic collisions

Luciano Rezzolla[1,2] **and Kentaro Takami**[1]

[1] Max-Planck-Institut für Gravitationsphysik, Albert Einstein Institut, Golm, Germany
[2] Department of Physics, Louisiana State University, Baton Rouge, LA, USA

E-mail: luciano.rezzolla@aei.mpg.de and kentaro.takami@aei.mpg.de

Abstract
Determining the conditions under which a black hole can be produced is a
long-standing and fundamental problem in general relativity. We use numerical
simulations of colliding self-gravitating fluid objects to study the conditions of
black-hole formation when the objects are boosted to ultrarelativistic speeds.
Expanding on the previous work, we show that the collision is characterized by
a type-I critical behaviour, with a black hole being produced for masses above
a critical value, M_c, and a partially bound object for masses below the critical
one. More importantly, we show for the first time that the critical mass varies
with the initial effective Lorentz factor $\langle \gamma \rangle$ following a simple scaling of the
type $M_c \sim K \langle \gamma \rangle^{-1.0}$, thus indicating that a black hole of infinitesimal mass
is produced in the limit of a diverging Lorentz factor. Furthermore, because a
scaling is present also in terms of the initial stellar compactness, we provide a
condition for black-hole formation in the spirit of the hoop conjecture.

PACS numbers: 04.25.Dm, 04.25.dk, 04.40.Dg, 95.30.Sf, 97.60.Jd, 97.60.Lf

(Some figures may appear in colour only in the online journal)

1. Introduction

There is little doubt that black-hole formation represents one of the most intriguing and
fascinating predictions of classical general relativity. There is abundant astronomical evidence
that black holes exist, and a number of considerations supporting the idea that under suitable
conditions gravitational collapse is inevitable [1]. In addition, there is overwhelming numerical
evidence that black-hole formation does take place in a variety of environments [2]. Yet, a
rigorous definition of the sufficient conditions for black-hole formation is still lacking. Hence,
it is not possible to predict whether the collision of two compact objects, either stars or
elementary particles, will lead to the formation of a black hole.

However, we are not without ideas and the intuitive *hoop conjecture* proposed by Thorne
in the 1970s, provides us with some reasonable guidelines [3]. We recall that the conjecture

states that a black hole is formed if an amount of 'mass–energy' E can be compressed to fit within a hoop with radius equal to or smaller than the corresponding Schwarzschild radius, i.e. if $R_{\text{hoop}} \leqslant R_{\text{s}} = 2GE/c^4$, where G is the gravitational constant and c the speed of light. Even though it can be made precise under particular circumstances [4], the hoop conjecture is not meant to be a precise mathematical statement and, in fact, it is difficult to predict if the above-mentioned collision will compress matter sufficiently to fit within the limiting hoop. Loosely speaking, what is difficult is to determine which part of the 'kinetic energy' of the system can be accounted to fit within the hoop. Since at the collision the conversion of kinetic energy into internal energy is a highly nonlinear process, any quantitative prediction becomes rapidly inaccurate as the speeds involved approach that of light.

As stated above, the hoop conjecture is purely classical. A quantum-mechanical equivalent is not difficult to formulate, although not very stringent, as it simply implies that a black hole will be formed at Planck-energy scales. The predicting power does not improve significantly when considering the conditions of black-hole formation in higher-dimensional theories of gravity (see, e.g. [5–7]). In these frameworks, the energy required for black-hole formation might be significantly smaller [5], thus providing the possibility of producing them in the Large Hadron Collider (LHC) [8], but no firm conclusion has been reached yet.

Clearly, although numerical simulations represent a realistic route to shed some light on this issue (see, e.g., [9–11]), even the simplest scenario of the collision of two compact objects at ultrarelativistic speeds is far from being simple and it is actually very challenging. The first step was taken by Eardley and Giddings [12], who have studied the formation of a black hole from the head-on collision of two plane-fronted gravitational waves with a nonzero impact parameter (previous work of D'Eath and Payne [13–15] using different methods had considered a zero impact parameter). In all of these analyses each incoming particle is modelled as a point particle accompanied by a plane-fronted gravitational shock wave corresponding to the Lorentz-contracted longitudinal gravitational field of the particle. At the instant of collision the two shock waves pass through one another and interact through nonlinear focusing and shearing. As a result of their investigation, a lower bound was set on the cross-section for black hole production, i.e. $\sigma > 32.5(GE/2c^4)^2$, where E is the centre-of-mass (lab) energy. More recently, and in a framework which is closer to the one considered here, this problem has been investigated by Choptuik and Pretorius [16], who studied the collision of two classical spherical solitons, with a total energy of the system in the lab frame $E = 2\gamma_{\text{b}}m_0c^2$, where m_0 is the 'rest-mass', $\gamma_{\text{b}} \equiv 1/\sqrt{1 - v_{\text{b}}^2/c^2}$ and v_{b} the boost velocity. They were then able to show that for collisions with sufficiently high boost, i.e. $\gamma_{\text{b}} \gtrsim 2.9$, a black hole can be formed.

In this work we report for the first time on black-hole production from the collision of two compact, self-gravitating, fluid objects boosted at ultrarelativistic speeds[3]. There are several important differences with the previous investigations in [13–15, 12, 16]. Differently from [13–15, 12], in fact, our colliding objects are not in vacuum and are not treated as point particles. Rather, our relativistic stars are obviously extended and self-gravitating objects, thus with a behaviour that is intrinsically different. Also, differently from [16], our objects are not described as scalar fields, but as fluids and thus represent a more realistic description of baryonic matter, such as the one employed when simulating relativistic heavy-ion collisions [18]. These intrinsic differences also make the comparison with the works of [13–15, 12] very hard if possible at all. On the other hand, many analogies exist with the collision of boson stars considered in [16], and that, as we will discuss below, can be interpreted within the more general description of black-hole production from ultrarelativistic collisions that we provide in this work.

---

[3] While this work was being reviewed, a similar investigation by East and Pretorius has also been reported [17].

Table 1. Initial properties of the isolated stars leading to supercritical models nearer to the critical line. Reported in the various columns are the central density ρ_c, the gravitational mass M, the rest-mass M_0, the radius R, the compactness M/R, the initial velocity and Lorentz factor v_b and γ_b and the corresponding effective value $\langle\gamma\rangle$ in units where $c = 1 = M_\odot$.

$\rho_c \times 10^4$	$M \times 10$	$M_0 \times 10$	$R \times 10^{-1}$	$(M/R) \times 10^2$	v_b	γ_b	$\langle\gamma\rangle$
5.316 13	8.970	9.348	1.101	8.148	0.30	1.048	1.033
4.900 00	8.501	8.837	1.111	7.653	0.50	1.155	1.107
3.750 00	7.043	7.267	1.140	6.179	0.70	1.400	1.284
3.000 00	5.947	6.103	1.160	5.126	0.80	1.667	1.497
2.500 00	5.142	5.257	1.174	4.379	0.86	1.960	1.757
2.050 00	4.362	4.443	1.187	3.674	0.90	2.294	2.116
1.200 00	2.728	2.759	1.213	2.248	0.95	3.202	3.618

Given these basic differences, it is not surprising that our results also show qualitative differences with respect to previous investigations. The most important of these differences is that we find that a black hole can be produced even from zero initial velocities if the initial masses are large enough; this behaviour is clearly absent in all previous results, where instead a critical initial boost is necessary [13–15, 12, 16]. In addition, we show that for each value of the effective Lorentz factor, $\langle\gamma\rangle$, a critical initial mass exists, M_c, above which a black hole is formed and below which matter, at least in part, self-gravitates. More importantly, both M_c follow a simple scaling with $\langle\gamma\rangle$.

2. Methodology

The numerical setup employed in our simulations is the *same* presented extensively in our previous works [19–21], and the interested reader can find in these references all the needed technical details. It is sufficient to recall here that we use an axisymmetric code to solve in two spatial dimensions, (x, z), the set of the Einstein and of the relativistic-hydrodynamic equations [19]. The axisymmetry of the spacetime is imposed exploiting the 'cartoon' technique, while the hydrodynamics equations are written explicitly in cylindrical coordinates. All the simulations use an ideal-gas EOS, $p = (\Gamma-1)\rho\epsilon$, where ρ is the rest-mass density, ϵ the specific internal energy and $\Gamma = 2$. The initial configurations consist of spherical stars, constructed as in [20, 21] after specifying the central density, ρ_c, where the latter also serves as a parameter to determine the critical model. The stars have an initial separation D and are boosted along the z-direction via a Lorentz transformation with boost v_b/c. To limit the initial violation in the constraints, D is chosen to be sufficiently large, i.e. $D = 240\,M_\odot$, and we use an optimal composition of the two isolated-star solutions that will be presented in a longer paper. The grid has uniform spacing $\Delta = 0.08(0.06)\,M_\odot$ with extents $x/M_\odot \in [0, 80]$ and $z/M_\odot \in [0, 150(200)]$, where the round brackets refer to the more demanding high-boost cases. Reflection boundary conditions are applied on the $z = 0$ plane, while outgoing conditions are used elsewhere. A summary of the initial properties of the isolated stars leading to supercritical models nearer to the critical line is presented in table 1.

3. Basic dynamics

The dynamics of the process is rather simple. As the two stars approach each other, the initial boost velocity increases as a result of the gravitational attraction, leading to a strong shock as the surfaces of the stars collide. In the case of *supercritical* initial data, i.e. of stars with
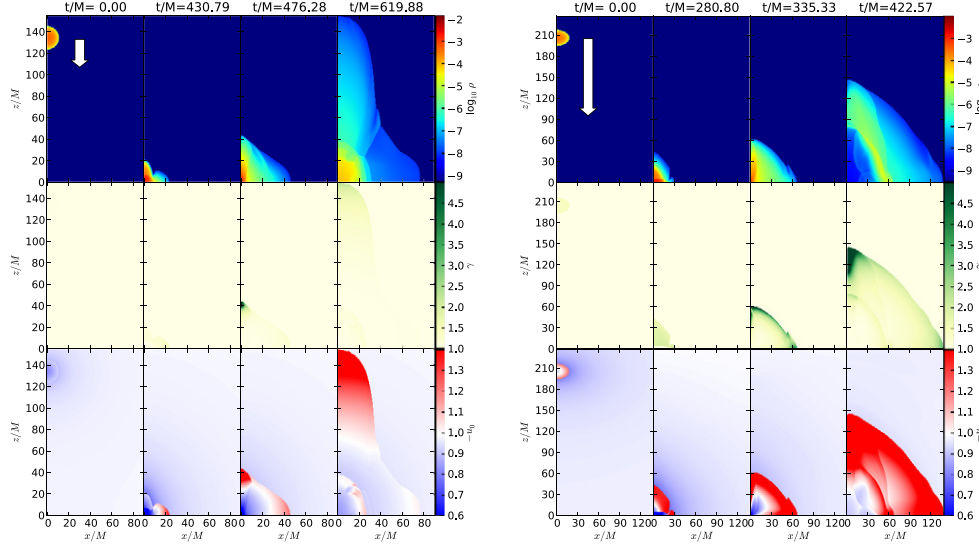
Class. Quantum Grav. **30** (2013) 012001   Fast Track Communication

IOP FTC ▶▶▶

Figure 1. Representative snapshots of the rest-mass density, ρ, in units where $c = 1 = M_\odot$ (top row), of the Lorentz factor, γ (middle row), and of the local fluid energy, $-u_0$ (bottom row), for subcritical models with an initial small boost $v_b/c = 0.3$ (left panel) or a large one $v_b/c = 0.8$ (right panel). Note that the post-collision flow is essentially jet-like for the low-boost case (left panel), while essentially spherical for the high-boost case (right panel); in this latter case, most of the matter is unbound.

masses above a critical value, M_c, a black hole is promptly produced and most of the matter is accreted. Conversely, in the case of *subcritical* initial data, i.e. of stars with masses below M_c, the product of the collision is a hot and extended object with large-amplitude oscillations. Part of the stellar matter is unbound and leaves the numerical grid as the product of the collision reaches an equilibrium.

Figure 1 shows snapshots at representative times of the rest-mass density, ρ (top row), of the Lorentz factor, $\gamma \equiv (1 - v^i v_i/c^2)^{-1/2}$ (middle row), and of the local fluid energy, $-u_0$ (bottom row), for two subcritical models. The left panel, in particular, refers to a binary boosted at $v_b/c = 0.3$. Note that the stars are strongly compressed by the collision, with the rest-mass density increasing exponentially. The merged object expand in a jet-like fashion along the z-direction, with the bulk of the matter being accelerated up to $\gamma \sim 16$, or equivalently, $v/c \sim 0.998$, but then settling on much slower flows with $\gamma \lesssim 2.1$. Furthermore, the front of the jet has $-u_0 > 1$ indicating that part of the shocked matter has sufficient energy to have become gravitationally unbound. As a result, the rest-mass density at the centre of the merged object is smaller than the maximum density of the initial configuration, although the origin still represents the region where the density is the largest. The right panel, on the other hand, refers to a highly boosted binary, i.e. with $v_b/c = 0.8$, with each star being initially highly distorted by the Lorentz contraction. Also in this case, the stars are strongly compressed by the collision, but the merged object expands in a spherical blast-wave fashion, with an almost spherical distribution of matter and bulk γ-factor. The latter reaches values as large as $\gamma \sim 30$, or equivalently, $v/c \sim 0.999$, which, in contrast with the low-boost case, do not decrease in time. It is worth emphasizing that these are the first calculations exploring such ultrarelativistic regimes in strong-curvature fields. As a comparison, the typical bulk Lorentz factor obtained
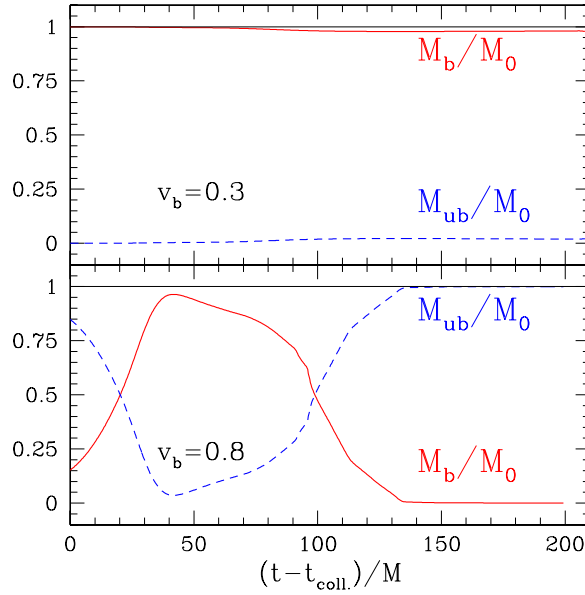
Figure 2. Evolution in collision-retarded time of the fraction of the matter which is unbound, M_{ub}/M_0 (blue dashed line), and the corresponding bound fraction M_b/M_0 (red solid line), defined as the complement to the total rest-mass M_0 (black solid line).

in the merger of binary neutron stars in quasi circular orbits is $\gamma \sim 1.03$ [22]. The very large kinetic energies involved in the collision are sufficient to make a very large portion of the stellar matter unbound, as clearly shown in the bottom-right panel of figure 1, which reports the local fluid energy. The rest-mass density distribution in the expanding blast wave has a minimum at the origin, where a large rarefaction is produced by the matter expanding as an ultrarelativistic thick shell.

The marked transition from a jet-like outflow, not too dissimilar from the simple Bjorken flow used to model the very early states of relativistic ion-collisions [23], to a shell-like structure, not too dissimilar from 'transverse expansion' modelled in the subsequent stages of relativistic ion-collisions (see [24] and references therein), signals that it is not unreasonable to extrapolate some of the results presented here also to the collision of ultrarelativistic elementary particles.

The transition from the two qualitatively different regimes discussed above is further confirmed by the evolution of the rest-mass normalized to the initial value M_0, which is shown in figure 2 for the low- (top panel) and high-boost (bottom panel) cases. More specifically, we show the fraction of the matter for which the local fluid energy $-u_0 > 1$ and which we therefore consider to be unbound, M_{ub}/M_0 (blue dashed line). We recall that $-u_0 > 1$ is a necessary but not sufficient condition for matter to be unbound, valid only in stationary spacetimes and ours never really are. However, this condition is probably also the only way to measure the fraction of unbound matter. Also shown is the corresponding bound fraction M_b/M_0 (red solid line), defined as the complement to the total rest-mass M_0 (black solid line), which is conserved essentially to machine precision. Note that this measurement is exact only in an axisymmetric and stationary spacetime, and therefore the estimates of M_{ub} and M_{ub} are sensible only in their asymptotic values. Clearly, the unbound fraction is just a few per cent of the total rest-mass in the case of a low-boost collision, with most of the matter being confined in

IOP FTC ▶▶▶

Class. Quantum Grav. **30** (2013) 012001   Fast Track Communication

the self-gravitating 'star'. This is to be contrasted with what happens for a high-boost collision, where the unbound fraction is ∼100% of the total rest-mass. This behaviour provides a strong indication that, at least for subcritical collisions, the role played by gravitational forces is a minor one as the kinetic energy is increased. This is what happens in the collision of two particles at ultrarelativistic speeds, where all of the matter is obviously unbound.

4. Critical behaviour and scaling

A remarkable property of the head-on collision of compact stars is the existence of type-I critical behaviour, which was first pointed out in [25] and subsequently extended in [19]. In essence, in these works it was found that when considering stars with initial zero velocity at infinity, it is possible to fine-tune the initial central density ρ_c (and hence the mass) near a critical value, $\rho_c^\star$, so that stars with $\rho_c > \rho_c^\star$ would collapse *eventually* to a black hole, while the models with $\rho_c < \rho_c^\star$ would *eventually* lead to a stable stellar configuration. As a result, the head-on collision of two neutron stars near the critical threshold can be seen as a transition in the space of configurations from an initial stable solution over to a critical metastable one which can either migrate to a stable solution or collapse to a black hole [21]. As the critical limit is approached, the survival time of the metastable object, τ_{eq}, increases as $\tau_{eq} = -\lambda \ln |\rho_c - \rho_c^\star|$, with $\lambda \sim 10$ [25, 19].

   Although the free-fall velocities considered in [25, 19] were very small, we find that the critical behaviour continues to hold also when the stars are boosted to ultrarelativistic velocities and that the threshold $\rho_c^\star$ is a function of the initial effective boost. It should be emphasized that determining $\rho_c^\star$ becomes especially challenging as the γ-factor is increased and the dynamics of the matter becomes extremely violent, with very strong shocks and rarefaction waves. However, we were able to determine the threshold for all the ranges of initial boosts considered, i.e. $v_b/c \in [0, 0.95]$, $\gamma_b \in [1, 3.2]$, and even to a reasonable accuracy, e.g. $\rho_c^\star = (3.288023 \pm 0.000003) \times 10^{14}\,\mathrm{g\,cm^{-3}}$, for the initial boost of $v_b/c = 0.3$.

   The existence of critical behaviour near which the details of the initial conditions become irrelevant and which is the *same* at different boosts, i.e. λ does not depend on γ nor on ρ_c ([25, 26] have shown that there is 'universality' when varying γ and fixing ρ_c), gives us a wonderful tool to explore the conditions of black-hole formation also far away from the masses and γ-factors considered in this communication. This is illustrated in figure 3, which reports the gravitational mass of the isolated spherical star as a function of the effective initial Lorentz factor

$$\langle \gamma \rangle \equiv \frac{\int dV\, T_{\mu\nu} n^\mu n^\nu}{(\int dV T_{\mu\nu} n^\mu n^\nu)_0}\,, \tag{1}$$

where $T_{\mu\nu}$ is the stress–energy tensor, n^μ is the unit normal to the spatial hyperspace with proper volume element dV and the index 0 refers to quantities measured in the initial unboosted frame. We note that we introduce the definition of an effective Lorentz factor (1) because the stars are extended and thus the γ-factor will be different in different parts of the star. Expression (1), on the other hand, can be taken as the ratio of the energies measured in the boosted and unboosted frames, and hence a generalization of the Lorentz factor for a point particle (indeed $\langle \gamma \rangle \rightarrow 1$ for $v_b \rightarrow 1$). Of course, other parametrizations are possible, still leading to scaling laws, but with slightly different exponents. An extended discussion of this point will be presented in a longer paper. Filled circles indicate initial data leading to a black hole, while triangles indicate initial data leading to a 'star', whereby we mean an object which is at least in part self-gravitating (orange errorbars provide an approximate upper limit of ∼ 8% to the error in the measurements). Also indicated as a blue solid line is the critical line separating the two

IOP FTC ▶▶▶

Class. Quantum Grav. **30** (2013) 012001   Fast Track Communication
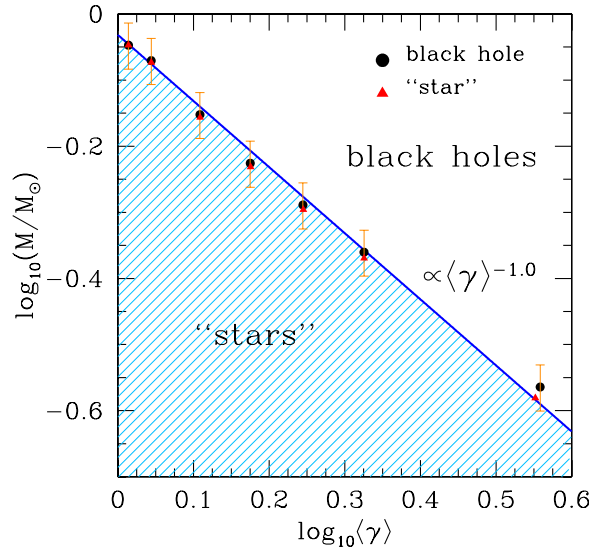

Figure 3. Critical line as a function of the effective Lorentz factor, with circles indicating black holes and triangles self-gravitating objects.

regions of black hole and star formation (the latter is shown as a shaded region). Clearly, the numerical results provide a tight fit of the critical line with a power law

$$M_c/M_\odot = K\langle\gamma\rangle^{-n} \approx 0.92\langle\gamma\rangle^{-1.03}, \tag{2}$$

and which represents the most interesting result of this work.

Expression (2) offers itself to a number of considerations. First, it essentially expresses the conservation of energy. Second, in the limit of zero initial velocities, $\langle\gamma\rangle \to 1$, we obtain that $M_c \simeq 0.92\,M_\odot$, so that the corresponding total mass, $2M_c$, is only $\sim 12\%$ larger than the maximum mass of the relative spherical-star sequence, i.e. $M_{max} = 1.637\,M_\odot$. Third, in the opposite limit of $\langle\gamma\rangle \to \infty$, expression (2) predicts that the critical mass will go zero. This is indeed what one would expect: as the kinetic energy diverges, no room is left for self-gravitating matter, which will all be ejected but for an infinitesimal amount which will go into building the zero-mass critical black hole. Fourthly, (2) is also in agreement with the results in [16, 17], whereby one can recognize the black-hole formation as the crossing of the critical line when moving to larger γ-factors while keeping the rest-mass constant. Finally, the scaling relation (2) can be expressed equivalently in terms of the original stellar compactness, M/R, as

$$(M/R)_c = K'\langle\gamma\rangle^{-n'} \approx 0.08\langle\gamma\rangle^{-1.13}. \tag{3}$$

Since $M_{lab} \equiv \langle\gamma\rangle M$ is the mass in the lab frame and R is the largest dimension in that frame being the transverse one to the motion, the ratio $(M_{lab}/R)_c = K'\langle\gamma\rangle^{1-n'} \approx K'\langle\gamma\rangle^{-0.13}$ provides the condition for the amount of energy that, when confined in a hoop of radius R, would lead to a black hole, as in the spirit of the hoop conjecture.

5. Conclusions

We have computed the first ultrarelativistic collisions of compact fluid stars leading to black-hole formation. The Lorentz factor reached in our relativistic-hydrodynamic simulations in

strong-field regimes are considerably larger than those ever explored in inspiralling neutron-star binaries. We find that the properties of the flow after the collision change with Lorentz factor, with most of the matter being ejected in a spherical blast wave for large boosts. As in the previous work, we find that the collision exhibits a critical behaviour of type I and that this persists also as the initial boost is increased. This allows us to use a simple scaling law with a transparent physical interpretation and a condition for black-hole formation in the spirit of the hoop conjecture.

Acknowledgments

References

[1] Wald R M 1984 *General Relativity* (Chicago: The University of Chicago Press)
[2] Rezzolla L, Giacomazzo B, Baiotti L, Granot J, Kouveliotou C and Aloy M A 2011 The missing link: merging neutron stars naturally produce jet-like structures and can power short gamma-ray bursts *Astrophys. J.* **732** L6
[3] Thorne K 1972 Nonspherical gravitational collapse: a short review *Magic Without Magic: John Archibald Wheeler* ed J Klauder (San Francisco: Freeman) p 231
[4] Senovilla J M M 2008 A reformulation of the hoop conjecture *Europhys. Lett.* **81** 20004
[5] Argyres P C, Dimopoulos S and March-Russell J 1998 Black holes and sub-millimeter dimensions *Phys. Lett.* B **441** 96–104
[6] Yoshino H and Nambu Y 2003 Black hole formation in the grazing collision of high-energy particles *Phys. Rev.* D **67** 024009
[7] Yoo C-M, Ishihara H, Kimura M and Tanzawa S 2010 Hoop conjecture and the horizon formation cross section in Kaluza–Klein spacetimes *Phys. Rev.* D **81** 024020
[8] Dimopoulos S and Landsberg G 2001 Black holes at the large hadron collider *Phys. Rev. Lett.* **87** 161602
[9] Sperhake U, Cardoso V, Pretorius F, Berti E and Gonzalez J A 2008 The high-energy collision of two black holes *Phys. Rev. Lett.* **101** 161101
[10] Shibata M, Okawa H and Yamamoto T 2008 High-velocity collision of two black holes *Phys. Rev.* D **78** 101501
[11] Sperhake U, Cardoso V, Pretorius F, Berti E, Hinderer T and Yunes N 2009 Cross section, final spin and zoom-whirl behavior in high-energy black-hole collisions *Phys. Rev. Lett.* **103** 131102
[12] Eardley D M and Giddings S B 2002 Classical black hole production in high-energy collisions *Phys. Rev.* D **66** 044011
[13] D'eath P D and Payne P N 1992 Gravitational radiation in black-hole collisions at the speed of light: I. Perturbation treatment of the axisymmetric collision *Phys. Rev.* D **46** 658–74
[14] D'eath P D and Payne P N 1992 Gravitational radiation in black-hole collisions at the speed of light: II. Reduction to two independent variables and calculation of the second-order news function *Phys. Rev.* D **46** 675–93
[15] D'eath P D and Payne P N 1992 Gravitational radiation in black-hole collisions at the speed of light: III. Results and conclusions *Phys. Rev.* D **46** 694–701
[16] Choptuik M W and Pretorius F 2010 Ultrarelativistic particle collisions *Phys. Rev. Lett.* **104** 111101
[17] East W E and Pretorius F 2012 Ultrarelativistic black hole formation arXiv:1210.0443
[18] Rischke D H, Bernard S and Maruhn J A 1995 Relativistic hydrodynamics for heavy-ion collisions: I. General aspects and expansion into vacuum *Nucl. Phys.* A **595** 346–82
[19] Kellerman T, Baiotti L, Giacomazzo B and Rezzolla L 2008 An improved formulation of the relativistic hydrodynamics equations in 2D Cartesian coordinates *Class. Quantum Grav.* **25** 225007
[20] Kellerman T, Rezzolla L and Radice D 2010 Critical phenomena in neutron stars: II. Head-on collisions *Class. Quantum Grav.* **27** 235016
[21] Radice D, Rezzolla L and Kellerman T 2010 Critical phenomena in neutron stars: I. Linearly unstable nonrotating models *Class. Quantum Grav.* **27** 235015

IOP FTC ▶▶▶

Class. Quantum Grav. **30** (2013) 012001   Fast Track Communication

[22] Rezzolla L, Baiotti L, Giacomazzo B, Link D and Font J A 2010 Accurate evolutions of unequal-mass neutron-star binaries: properties of the torus and short GRB engines *Class. Quantum Grav.* **27** 114105

[23] Bjorken J D 1983 Highly relativistic nucleus–nucleus collisions: the central rapidity region *Phys. Rev.* D **27** 140–51

[24] Huovinen P and Ruuskanen P V 2006 Hydrodynamic models for heavy ion collisions *Annu. Rev. Nucl. Part. Sci.* **56** 163–206

[25] Jin K-J *et al* 2007 Critical phenomena in head-on collision of neutron stars *Phys. Rev. Lett.* **98** 131101

[26] Wan M-B 2011 Universality and properties of neutron star type I critical collapses *Class. Quantum Grav.* **28** 155002